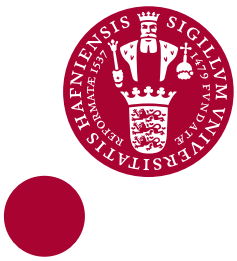

The lower Maastrichtian Hvidskud succession, Møns Klint, Denmark

calcareous nannofossil biostratigraphy, carbon isotope stratigraphy, and bulk and brachiopod oxygen isotopes

Jelby, Mads Engholm; Thibault, Nicolas; Surlyk, Finn; Ullmann, Clemens V.; Harlou, Rikke; Korte, Christoph

Published in:
Bulletin of the Geological Society of Denmark

Publication date:
2014

Document version
Publisher's PDF, also known as Version of record

The lower Maastrichtian Hvidskud succession, Møns Klint, Denmark: calcareous nannofossil biostratigraphy, carbon isotope stratigraphy, and bulk and brachiopod oxygen isotopes

MADS ENGHOLM JELBY, NICOLAS THIBAULT, FINN SURLYK, CLEMENS V. ULLMANN, RIKKE HARLOU & CHRISTOPH KORTE

Jelby, M.E., Thibault, N., Surlyk, F., Ullmann, C.V., Harlou, R. & Korte, C. 2014: The lower Maastrichtian Hvidskud succession, Møns Klint, Denmark: calcareous nannofossil biostratigraphy, carbon isotope stratigraphy, and bulk and brachiopod oxygen isotopes. © 2014 by Bulletin of the Geological Society of Denmark, Vol. 62, pp. 89–104. ISSN 2245-7070. (www.2dgf.dk/publikationer/bulletin).

A new calcareous nannofossil and $\delta^{13}C$ stratigraphy is established for the chalk exposed in the lower Maastrichtian Hvidskud succession, Møns Klint, Denmark. It is based on 21 nannofossil samples and analysis of 82 stable isotope samples, allowing correlation with a previously established brachiopod zonation. The succession, which belongs to the brachiopod *spinosa-subtilis* to *pulchellus-pulchellus* zones, extends upwards from calcareous nannofossil subzone UC16ii to UC19ii and encompasses $\delta^{13}C$ events M1+ to M2+. A new chronostratigraphic and geochronological age model is proposed based on correlation with the cored boreholes Stevns-1 (Denmark) and ODP Site 762C (Indian Ocean). Hvidskud encompasses the 405 kyr eccentricity cycles $Ma_{405}13 – Ma_{405}11$ within magnetochron C31r. A sedimentation rate of 5.0 cm kyr^{-1} can be inferred from correlation to geochronological tie-points in ODP 762C, suggesting an age of ~70.9 Ma for the base of the succession and a duration of >680 kyr for the investigated interval. The Hvidskud succession is well-exposed, easily accessible, and the new stratigraphic framework and precise age model suggest that it can be used as a key locality for stratigraphic correlation of the lower Maastrichtian in north-western Europe. Information on palaeo-seawater temperatures can be drawn from oxygen isotope records obtained from bulk rock samples and 24 micromorphic brachiopod specimens (*Terebratulina faujasii*). The brachiopod data show a clear diagenetic trend but point to an upper range of unaltered values between –0.4 and –0.6‰. Assuming a $\delta^{18}O$ value of –1‰ for seawater in a Cretaceous ice-free world, this would indicate bottom water temperatures of 13.6 to 14.3°C of the Danish Chalk Sea (45°N) during the early Maastrichtian cooling.

Keywords: lower Maastrichtian, calcareous nannofossil biostratigraphy, $\delta^{13}C$ stratigraphy, Danish Basin, brachiopod zonation, oxygen isotopes, Hvidskud.

Mads Engholm Jelby [madsjelby@hotmail.com], Nicolas Thibault [nt@ign.ku.dk], Finn Surlyk [finns@ign.ku.dk], Clemens V. Ullmann [cu@ign.ku.dk], Rikke Harlou [rikke@harlou.dk], Christoph Korte [korte@ign.ku.dk], Department of Geosciences and Natural Resource Management, University of Copenhagen, Øster Voldgade 10, DK-1350 Copenhagen K, Denmark.

Received 13 May 2014
Accepted in revised form
31 October 2014
Published online
28 November 2014

The coastal cliff Møns Klint, situated in eastern Denmark at the south-eastern margin of the Danish Basin, is an important locality for the study of the Maastrichtian of northern Europe (Fig. 1). The 6 km long and up to 130 m high cliff is composed of large glaciotectonic thrust sheets of white chalk and Quaternary deposits.

The Hvidskud thrust sheet, situated in the southern part of the cliff, exposes the thickest succession at Møns Klint comprising *c.* 60 m of lower Maastrichtian white chalk with flint bands and nodules, and abundant *Thalassinoides* burrows (Figs 2, 3). Previous stratigraphic studies of the succession are based on foraminifera, coccoliths, dinoflagellates, belemnites and brachiopods (Birkelund 1957; Steinich 1965; Surlyk 1970, 1979, 1982, 1984; Surlyk & Birkelund 1977; Schulz 1979). In particular, a detailed zonation was established on the basis of micromorphic brachiopods obtained from washed bulk samples (Surlyk 1969, 1970, 1979, 1982, 1984). Many of these species have a limited vertical distribution, occur in great numbers

and have proved to be useful for biostratigraphic zonation and correlation of the chalk in north-western Europe (Steinich 1965; Surlyk 1970, 1984; Johansen & Surlyk 1990).

Many of the stratigraphically important microfossils from low latitudes are either absent or rare in the Maastrichtian chalk of north-western Europe, making it difficult to correlate precisely the Danish Maastrichtian brachiopod zonation with the newest Maastrichtian time scale (Thibault *et al.* 2012a, b). Recently, the Danish Maastrichtian has been correlated with the $\delta^{13}C$ stratigraphy and calcareous nannofossil biostratigraphy of north-western Europe (Voigt *et al.* 2010, 2012; Thibault *et al.* 2012a, b; Surlyk *et al.* 2013).

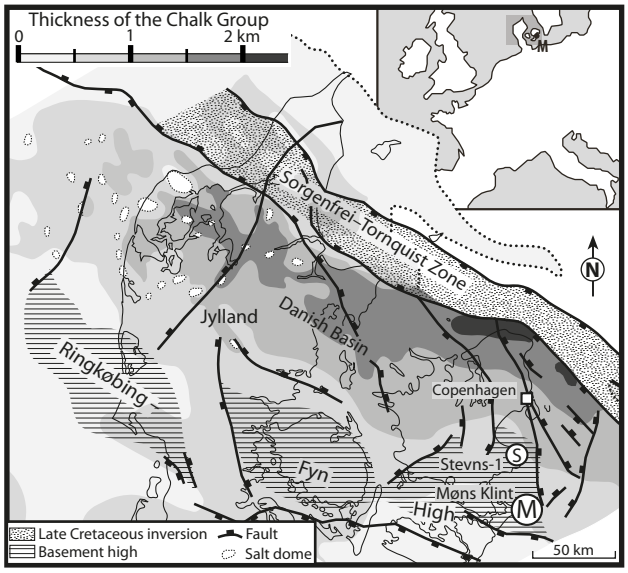

Fig. 1. Map of the Danish Basin showing the thickness of the Upper Cretaceous – Danian Chalk Group. Circled M, Møns Klint; Circled S, Stevns-1 drill hole. Modified from Stemmerik *et al.* (2006).

Fig. 2. Photograph of the upper part of the Hvidskud succession, Møns Klint, exposing glacially thrusted lower Maastrichtian white chalk with bands and nodules of black flint. Person standing next to the prominent flint band at 25.5 m, *c.* 8.5 m below the thin hardground.

Along with the development of an astronomical Maastrichtian time scale (Husson *et al.* 2011; Thibault *et al.* 2012b), this allows the establishment of an age model for the Hvidskud succession within the framework of the $\delta^{13}C$ and nannofossil stratigraphies established for the Danish lower Maastrichtian.

The aim of the study is to establish a new calcareous nannofossil and $\delta^{13}C$ stratigraphy for the Hvidskud succession and to correlate these data with the brachiopod zonation of Surlyk (1984). An age model is proposed for the Hvidskud succession based on these results combined with $\delta^{13}C$ and nannofossil data for north-western Europe (Voigt *et al.* 2010, 2012; Thibault *et al.* 2012a, b) and the new astronomical time scale for the Maastrichtian (Husson *et al.* 2011; Thibault *et al.* 2012b). Additionally, climatic implications can be drawn for bottom waters of the lower Maastrichtian in the Danish Basin based on new isotopic results from micromorphic brachiopods.

Regional setting and stratigraphy

The Danish Basin is NW–SE elongated and is limited to the NE by the inverted and faulted Sorgenfrei–Tornquist Zone and to the S by the Ringkøbing–Fyn High. Møns Klint is situated over the eastern end of the high (Fig. 1). During the Cretaceous the basin was characterised by regional subsidence, interrupted by phases of inversion and relative uplift of the Sorgenfrei–Tornquist Zone (Liboriussen *et al.* 1987; Håkansson & Surlyk 1997; Vejbæk & Andersen 2002; Mogensen & Korstgård 2003). The Late Cretaceous experienced an ongoing sea-level rise, culminating in one of the globally highest sea-level stands during the Phanerozoic, resulting in the flooding of much of northern Europe (e.g. Haq *et al.* 1988; Kominz *et al.* 2008). The chalk, which is essentially a pelagic sediment, was deposited throughout the late Cenomanian to Maastrichtian, and the Campanian–Maastrichtian interval reaches thicknesses of up to several hundreds of metres in the Danish Basin (Stenestad 1972; Surlyk & Lykke-Andersen 2007; Rasmussen & Surlyk 2012; Surlyk *et al.* 2013). Monotonous, benthos-poor chalk was deposited in relatively deep water in the central parts of the basin. On the other hand, abundant minor omission surfaces and rich benthic fossil assemblages in parts of the Maastrichtian chalk of Møns Klint, including the Hvidskud succession, indicate that deposition occurred in relatively shallower water above the Ringkøbing–Fyn High, however still well below the photic zone and storm wave base (Fig. 3; Surlyk & Birkelund 1977).

The Hvidskud succession comprises the *spinosa-*

Table 1. Stratigraphic heights of brachiopod bio-events (first occurrences, FOs) in the Hvidskud succession, Møns Klint. Heights from Surlyk (1979).

Bio-events (FOs)	m	Maastrichtian substage	Brachiopod zones (Surlyk 1984)
Trigonosemus pulchellus	31.5	Base upper lower	*pulchellus-pulchellus*
Terebratulina subtilis	22.7	lower lower	*subtilis-pulchellus*

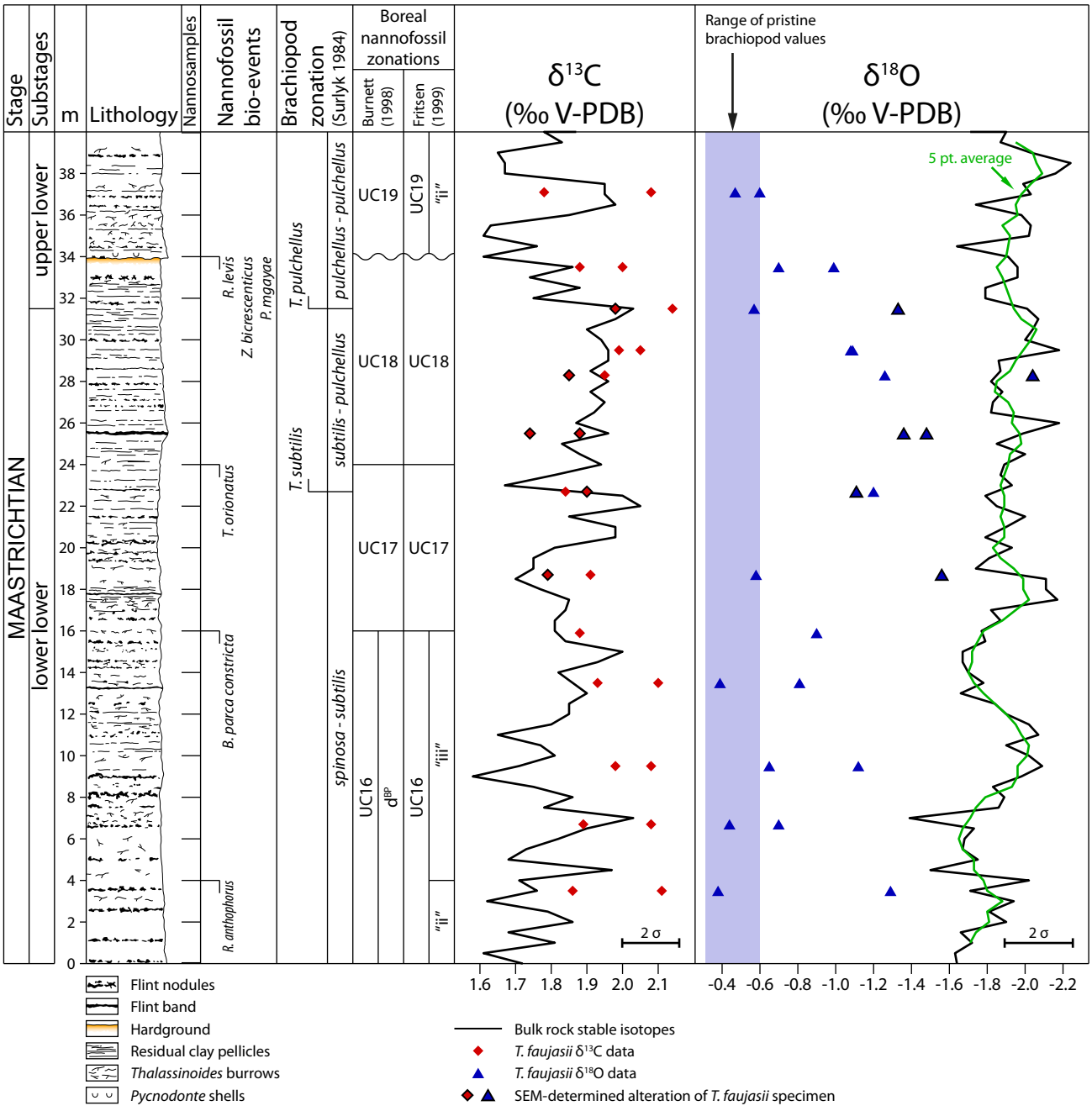

Fig. 3. Correlation of brachiopod and nannofossil zonations with bulk rock stable isotope profiles of the Hvidskud succession together with stable isotope data from the micromorphic brachiopod *Terebratulina faujasii*. Calcareous nannofossil and stable isotope data from this study. The range of pristine brachiopod $\delta^{18}O$ values represents the least altered signal for bottom water conditions and may thus be used to estimate the minimum palaeotemperature of bottom waters of the Chalk Sea in the Danish Basin. Note the relatively light stable isotope values of the brachiopod specimens considered to be altered from SEM inspection. Error bars represent the reproducibility (2σ) of in-house reference material. Log after Surlyk & Birkelund (1977).

subtilis, *subtilis-pulchellus* and *pulchellus-pulchellus* brachiopod zones of Surlyk (1984). The base of the *pulchellus-pulchellus* zone defines the boundary between the lower lower and the upper lower Maastrichtian in the Boreal Realm (Table 1; Surlyk 1969, 1970).

Material and methods

The measured section of Surlyk (1970, 1984) was extended downwards by *c.* 3.5 m and upwards by 1 m, resulting in a total thickness of 40 m. The exposed succession in the cliff is *c.* 60 m thick but the lower part is tectonically disturbed and was not included in the study. Nannoplankton biostratigraphy and stable isotope analyses were based on 82 samples with a resolution of 50 cm (Tables 2, 3). In addition, stable isotope, trace element and scanning electron microscope (SEM) analyses were performed on micromorphic brachiopods (Table 4) from the collection of F. Surlyk in order to synthesise climatic implications from both planktonic and benthic species.

Sample preparation

Bulk samples were dried at 40°C for 48 hours in order to extract possible interstitial fluids from the chalk.

Preparation of microbrachiopods

In order to retrieve monospecific stable isotope and trace element signals, 24 micromorphic brachiopods (distributed over 13 sample levels) of the species *Terebratulina faujasii* were prepared. This species was chosen for analysis as it occurs throughout the succession. Two samples were prepared for each stratigraphic level with one exception where the amount of shell material only allowed preparation of a single sample (Table 4). Articulate brachiopod shells are composed of an outer finely granular primary layer and an interior fibrous or lamellar secondary layer, both consisting of low-Mg calcite (e.g. Griesshaber *et al*. 2007). They may develop an additional prismatic tertiary layer (Parkinson *et al.* 2005). The secondary layer is very resistant to diagenesis (e.g. Veizer *et al.* 1999; Korte *et al.* 2008), and it has been documented that this layer, in contrast to the primary layer, is commonly precipitated in or close to isotopic equilibrium with seawater (Carpenter & Lohmann 1995; Parkinson *et al.* 2005). In order to remove the primary layer and possible attached chalk from the brachiopod shells, the following method was developed by R. Harlou at the Department of Geosciences and Natural Resource Management, University of Copenhagen. The brachiopod shells were carefully cleaned by alternate leaching with 1M acetic acid (CH_3COOH) and cleaning/neutralising with deionised water (MilliQ H_2O).

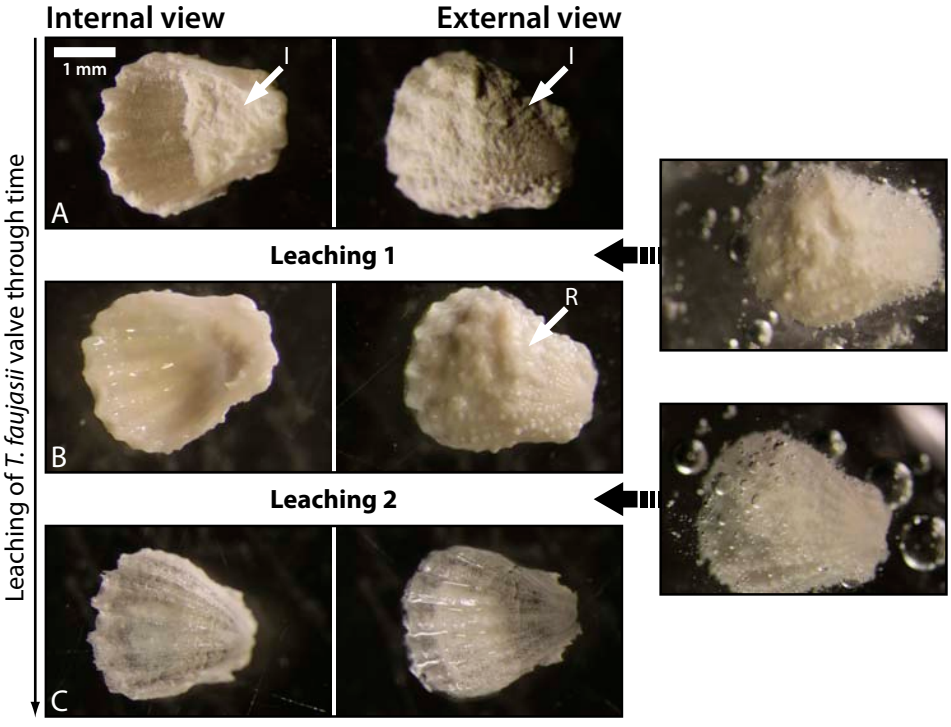

Fig. 4. Representative pictures of the multi-stepped leaching process developed by R. Harlou at the Department of Geosciences and Natural Resource Management, University of Copenhagen. The example presented here is a dorsal valve from the micromorphic brachiopod *Terebratulina faujasii*. Both external and internal views of the valve are included in order to ease comparison between each step. Note how the valve is progressively cleaned throughout the leaching process. **A**: The initial condition with adhering chalk (I) on both the internal and external sides of the valve. **B**: A cleaner valve after the first leaching with only residual chalk (R) on the external side of the valve. **C**: The outer primary layer has been removed from the valve after the second leaching. 1 mm scale bar applies to all pictures. Sample A4 (1), 33.5 m.

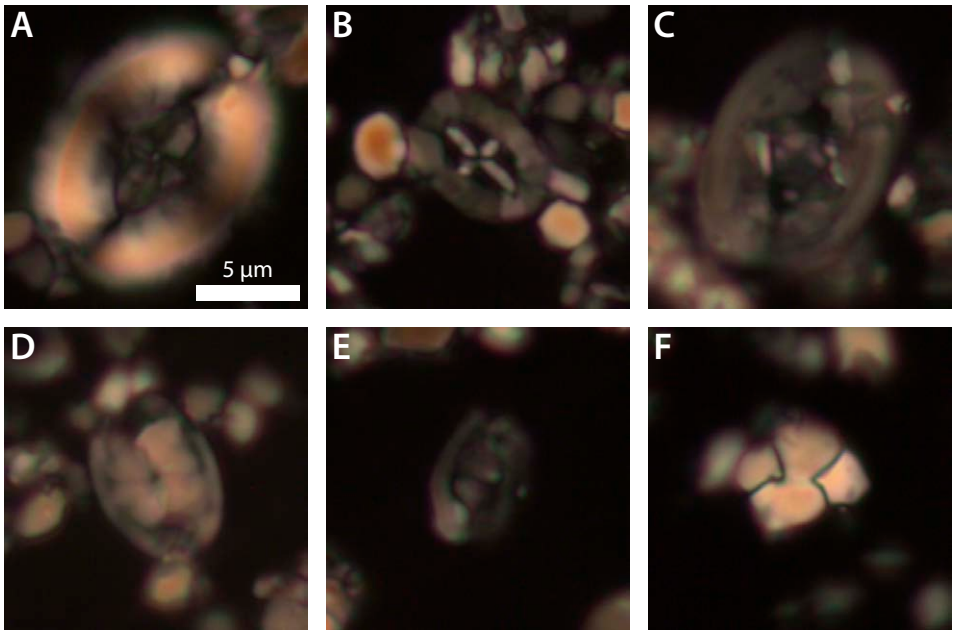

Fig. 5. Main calcareous nannofossils used for biostratigraphic subdivision of the Hvidskud succession, Møns Klint (A–E), and an additional important species found in the succession (F). **A**: *Broinsonia parca constricta*, 14.0 m. **B**: *Prediscosphaera mgayae*, 24.0 m. **C**: *Reinhardtites levis*, 8.0 m. **D**: *Tranolithus orionatus*, 24.0 m. **E**: *Zeugrhabdotus bicrescenticus*, 6.0 m. **F**: *Calculites obscurus*, 0.0 m. 5 µm scale bar applies to all pictures.

The latter also stopped the process of leaching if added in excess. This treatment is excellent for cleaning the shell surfaces and removing the primary layers of articulate brachiopods when preparing for isotope measurements (Fig. 4). The shells were subsequently dried at 40°C for 24 hours in order to extract residual interstitial fluids from the carbonate.

Calcareous nannofossil biostratigraphy

Dried bulk samples were gently disaggregated in a mortar and 50 mg (±0.5 mg) of the treated sediment was dispersed in 50 ml of deionised water buffered with diluted ammonium to avoid dissolution. The suspension was homogenised by treating it in an ultrasonic bath for 10 s and subsequently stirred with a magnet before aliquots of 0.75 ml of the suspension were evenly distributed on microscope slides by using a micropipette (see Koch & Young 2007). A total of 21 slides were produced, covering the complete succession and representing a stratigraphic resolution of 2 m.

Stratigraphic distribution

A semiquantitative analysis of the stratigraphic distribution of calcareous nannofossils was performed (Table 2) based on counting of species abundances (randomly counting of specimens at a magnification of ×1600). Counting was performed on >150 fields of view (FOVs) for each microscope slide. Counts were determined as follows: a species is common (C) if one to 10 specimens were observed in each FOV; there are few (F) if one specimen was observed in every two to 10 FOVs; a species is rare (R) if one specimen was observed in 11 to 100 FOVs and very rare (VR) if one specimen was observed in 100 to 200 FOVs; single (S) means that only one specimen was observed during the entire investigation of a single slide. The nannofossil biozonations are established using the last occurrence (LO) of key nannofossil markers (Fig. 5; Table 2). The biozonations of Burnett (1998) and Fritsen (1999) are applied (Fig. 6).

The Upper Cretaceous chalk of the North Sea and Danish Basin suffered from considerable redeposi-

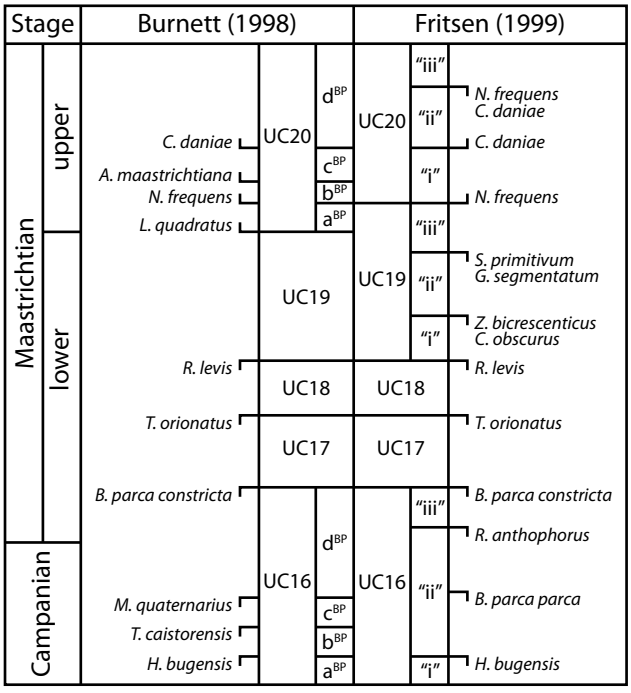

Fig. 6. Main nannofossil bio-events and biozonation schemes of Burnett (1998) and Fritsen (1999) for the upper Campanian – Maastrichtian of the Boreal Realm.

tion (e.g. Esmerode *et al*. 2008; Anderskouv & Surlyk 2011), suggesting that the precision of first and last occurrences of calcareous nannofossil markers may sometimes be disturbed and lead to uncertainties (Thibault *et al*. 2012a). Single spotty occurrences were therefore discarded as these are more likely to be reworked than *in situ*. Additional FOVs, up to an entire traverse of a slide, were examined to document rare species. Three modes of preservation of calcareous nannofossils (very poor, poor and good) have been considered, using the visual criteria of Roth (1983) for etching and overgrowth.

Stable isotope analyses

Approximately 200 to 900 μg of brachiopod shell fragments and bulk rock carbonate samples were transferred into glass vials (3.5 ml), sealed with rubber septa, and flushed with clean helium for 240 s. The aliquots were subsequently treated with ~0.05 ml anhydrous orthophosphoric acid (>100%) and equilibrated for >100 min at 70°C using a multiflow unit. The resultant CO_2 was analysed for carbon and oxygen isotopic compositions using the Micromass Iso Prime Isotope Ratio Mass Spectrometer at the Department of Geosciences and Natural Resource Management, University of Copenhagen. The raw data were corrected for weight dependent effects by measuring the Copenhagen in-house reference material (LEO: Carrara marble), covering the weight ranges of the analysed sample sets. Carbon and oxygen isotope values are expressed in per mil relative to the V-PDB reference (Tables 3, 4). The reproducibility (2sd) of the analysis, controlled by multiple measurements of the in-house reference material, was 0.18‰ for oxygen and 0.08‰ for carbon over a period of one year (2011, n = 649). For more analytical details see Ullmann *et al.* (2013).

Table 2. Distribution chart of selected calcareous nannofossil bio-events (last occurrences) in the Hvidskud succession, Møns Klint

Sample numbers	*Stratigraphic height (m)*	*Prediscosphaera stoveri*	*Kamptnerius magnificus*	*Arkhangelskiella cymbiformis* var. N	*Calculites obscurus*	*Biscutum coronum*	*Biscutum magnum*	*Zeugrhabdotus bicrescenticus*	*Reinhardtites levis*	*Prediscosphaera mgayae*	*Tranolithus orionatus*	*Broinsonia parca constricta*	*Reinhardtites anthophorus*	Preservation	UC Zones	
															Burnett (1998)	Fritsen (1999)
81	40	C	F	F	R		R			S				P	UC19	UC19ii
77	38	R	F	R	R		R							VP	UC19	UC19ii
73	36	R	C	R			R							VP	UC19	UC19ii
69	34	F	F	F	R			F	R	R				VP	UC18	UC18
65	32	F	F	R				C	R					VP	UC18	UC18
61	30	F	F	R	R			F	R	R				P	UC18	UC18
57	28	F	C	F				C	R	F				G	UC18	UC18
53	26	C	F	R				C	F	F				P	UC18	UC18
49	24	F	C	R				C	R	R	R			P	UC17	UC17
45	22	F	F	F				C	F	R				G	UC17	UC17
41	20	F	C	R				C	R	F				G	UC17	UC17
37	18	F	F	F				R	R	S				G	UC17	UC17
33	16	C	F	C				F	R	F		R		G	UC16d	16iii
29	14	F	F	R					F	R	R	R		G	UC16d	16iii
25	12	C	F	R	R		R	R	F			VR		G	UC16d	16iii
21	10	F	F	F	R		F	F	F	VR				G	UC16d	16iii
17	8	F	F	C	F		R	C	F	VR				G	UC16d	16iii
13	6	R	C	F	R		R	F	R	R				VP	UC16d	16iii
9	4	C	F	F	R		R	F	F	R			R	P	UC16d	16ii
5	2	C	R	F	R		R	R	R	R			R	G	UC16d	16ii
1	0	R	F	R	F	VR	VR	F		R		R		G	UC16d	16ii

C, Common (= 1–10 specimens/FOV); F, Few (= 1 specimen/2–10 FOVs); R, Rare (1 specimen/11–100 FOVs); VR, Very Rare (1 specimen/100–200 FOVs); S, Single specimen

Brachiopod element ratios

Remains of the reacted sample aliquots from the mass spectrometric analysis were used for element ratio measurements of the brachiopod shells. All samples were diluted to a nominal Ca concentration of 25 μg/g using 2% HNO_3. Samples were measured using a Perkin Elmer Optima 7000 DV ICP-OES at the Department of Geosciences and Natural Resource Management, University of Copenhagen, using a

Table 3. Bulk rock stable isotope data and stratigraphic position of samples

Height (m)	Maastrichtian substage	Boreal nannofossil zonations		$\delta^{13}C$ (‰ V-PDB)	$\delta^{18}O$ (‰ V-PDB)
		Burnett (1998)	Fritsen (1999)		
40.0	upper lower	UC19	UC19ii	1.87	–1.71
40.0	upper lower	UC19	UC19ii	1.78	–1.90
39.5	upper lower	UC19	UC19ii	1.83	–1.87
39.0	upper lower	UC19	UC19ii	1.65	–2.03
38.5	upper lower	UC19	UC19ii	1.67	–2.24
38.0	upper lower	UC19	UC19ii	1.67	–2.16
37.5	upper lower	UC19	UC19ii	1.95	–1.99
37.0	upper lower	UC19	UC19ii	1.95	–2.03
36.5	upper lower	UC19	UC19ii	1.98	–1.74
36.0	upper lower	UC19	UC19ii	1.85	–1.98
35.5	upper lower	UC19	UC19ii	1.63	–2.03
35.0	upper lower	UC19	UC19ii	1.61	–2.02
34.5	upper lower	UC19	UC19ii	1.76	–1.64
34.0	upper lower	Base UC19	Base UC19ii	1.61	–1.91
33.5	upper lower	UC18	UC18	1.86	–1.96
33.0	upper lower	UC18	UC18	1.74	–1.96
32.5	upper lower	UC18	UC18	1.88	–1.79
32.0	upper lower	UC18	UC18	1.75	–1.79
31.5	Base upper lower	UC18	UC18	2.03	–2.01
31.0	lower lower	UC18	UC18	1.98	–2.07
30.5	lower lower	UC18	UC18	1.90	–2.04
30.0	lower lower	UC18	UC18	1.94	–2.00
29.5	lower lower	UC18	UC18	1.96	–2.18
29.0	lower lower	UC18	UC18	1.96	–1.86
28.5	lower lower	UC18	UC18	1.91	–1.87
28.0	lower lower	UC18	UC18	1.96	–1.82
27.5	lower lower	UC18	UC18	1.91	–1.88
27.0	lower lower	UC18	UC18	1.95	–1.83
26.5	lower lower	UC18	UC18	1.92	–1.82
26.0	lower lower	UC18	UC18	1.87	–2.18
25.5	lower lower	UC18	UC18	1.96	–1.99
25.0	lower lower	UC18	UC18	1.83	–1.85
24.5	lower lower	UC18	UC18	1.88	–2.00
24.0	lower lower	Base UC18	Base UC18	1.94	–1.89
23.5	lower lower	UC17	UC17	1.81	–1.87
23.0	lower lower	UC17	UC17	1.67	–1.93
22.5	lower lower	UC17	UC17	2.00	–1.79
22.0	lower lower	UC17	UC17	2.05	–1.85
21.5	lower lower	UC17	UC17	1.85	–2.00
21.0	lower lower	UC17	UC17	1.98	–1.90
20.5	lower lower	UC17	UC17	1.98	–1.79
20.0	lower lower	UC17	UC17	1.81	–1.93
19.5	lower lower	UC17	UC17	1.75	–1.81
19.0	lower lower	UC17	UC17	1.75	–1.74
18.5	lower lower	UC17	UC17	1.70	–2.11
18.0	lower lower	UC17	UC17	1.77	–2.11
17.5	lower lower	UC17	UC17	1.85	–2.17
17.0	lower lower	UC17	UC17	1.84	–1.82
16.5	lower lower	UC17	UC17	1.81	–1.87
16.0	lower lower	Base UC17	Base UC17	1.81	–1.77
15.5	lower lower	UC16d^{BP}	UC16iii	1.84	–1.79
15.0	lower lower	UC16d^{BP}	UC16iii	2.00	–1.67
14.5	lower lower	UC16d^{BP}	UC16iii	1.93	–1.67
14.0	lower lower	UC16d^{BP}	UC16iii	1.82	–1.70
13.5	lower lower	UC16d^{BP}	UC16iii	1.86	–1.78
13.0	lower lower	UC16d^{BP}	UC16iii	1.90	–1.66
12.5	lower lower	UC16d^{BP}	UC16iii	1.85	–1.84
12.0	lower lower	UC16d^{BP}	UC16iii	1.85	–1.90
11.5	lower lower	UC16d^{BP}	UC16iii	1.80	–2.02
11.0	lower lower	UC16d^{BP}	UC16iii	1.65	–2.07
10.5	lower lower	UC16d^{BP}	UC16iii	1.77	–1.90
10.0	lower lower	UC16d^{BP}	UC16iii	1.81	–2.02
9.5	lower lower	UC16d^{BP}	UC16iii	1.71	–2.09
9.0	lower lower	UC16d^{BP}	UC16iii	1.58	–1.98
8.5	lower lower	UC16d^{BP}	UC16iii	1.75	–1.83
8.0	lower lower	UC16d^{BP}	UC16iii	1.86	–1.89
7.5	lower lower	UC16d^{BP}	UC16iii	1.78	–1.86
7.0	lower lower	UC16d^{BP}	UC16iii	2.03	–1.39
6.5	lower lower	UC16d^{BP}	UC16iii	1.90	–1.73
6.0	lower lower	UC16d^{BP}	UC16iii	1.82	–1.68
5.5	lower lower	UC16d^{BP}	UC16iii	1.73	–1.67
5.0	lower lower	UC16d^{BP}	UC16iii	1.68	–1.75
4.5	lower lower	UC16d^{BP}	UC16iii	1.97	–1.50
4.0	lower lower	UC16d^{BP}	Base UC16iii	1.71	–2.02
3.5	lower lower	UC16d^{BP}	UC16ii	1.76	–1.71
3.0	lower lower	UC16d^{BP}	UC16ii	1.62	–1.94
2.5	lower lower	UC16d^{BP}	UC16ii	1.79	–1.81
2.0	lower lower	UC16d^{BP}	UC16ii	1.86	–1.90
1.5	lower lower	UC16d^{BP}	UC16ii	1.68	–1.66
1.0	lower lower	UC16d^{BP}	UC16ii	1.81	–1.72
0.5	lower lower	UC16d^{BP}	UC16ii	1.61	–1.63
0.0	lower lower	UC16d^{BP}	UC16ii	1.72	–1.64

three-point calibration of matrix matched and synthetic calibration solutions. Accuracy and reproducibility were controlled by multiple measurements of the reference materials JDo-1 (dolostone) and JLs-1 (limestone). Reproducibilities (2sd) of the analyses are better than 2.6% for Mg/Ca and better than 2.2% for Sr/Ca. Reproducibility of Mn/Ca is 2.8% for JDo-1 (~150 μmol/mol) and 8.0% for JLs-1 (~29 μmol/mol). Measured ratios agree with ratios calculated by Imai *et al.* (1996) within 2%, apart from Mg/Ca in JLs-1, which was measured to be 8% lower.

SEM screening of micromorphic brachiopods

A total of 20 pieces of brachiopod shells were coated in gold and optically checked using the FEI Quanta 250 SEM of the Natural History Museum of Denmark, University of Copenhagen, in order to identify potential textural alteration. Photographs were taken of general and peculiar features representative of each sample (Fig. 7). The preservation state of the secondary shell layers was of particular interest. In addition, it was checked whether the primary layers were completely removed by leaching. The shell fragments were therefore extracted after the leaching process. Due to lack of material, SEM investigations were not possible for certain specimens (Table 4).

Results

Nannofossil bio-events, biozonations and preservation

Most of the investigated samples exhibit moderate preservation with little etching and some diagenetic overgrowth. However, samples from the uppermost part of the succession (from 30.0 m up-section) exhibit poor to very poor preservation. Nannofossil counting was performed on 12 key coccolith species (Fig. 5; Table

Table 4. Micromorphic brachiopod (*Terebratulina faujasii*) stable isotope, trace element and SEM data

Samples	Additional specimen prepared	SEM inspection	SEM-determined alteration	Height (m)	$\delta^{13}C$ (‰ V-PDB)	$\delta^{18}O$ (‰ V-PDB)	Mg/Ca (mmol/mol)	Sr/Ca (mmol/mol)	Mn/Ca (μmol/mol)
A2 (1)		×		37.1	1.78	–0.60	10.6	1.21	124
A2 (2)				37.1	2.08	–0.47	10.8	1.25	114
A4 (1)				33.5	1.88	–0.99	10.0	1.15	138
A4 (2)	×	×		33.5	2.00	–0.70	10.6	1.26	92
A5 (1)		×		31.5	2.14	–0.57	9.8	1.35	76
A5 (2)	×	×	×	31.5	1.98	–1.33	9.9	1.03	147
A6 (1)		×		29.5	2.05	–1.08	9.6	1.29	90
A6 (2)	×	×		29.5	1.99	–1.09	9.9	1.20	111
A7 (1)		×	×	28.3	1.85	–2.04	9.3	0.96	148
A7 (2)	×	×		28.3	1.95	–1.26	10.0	1.23	106
A9 (1)		×	×	25.5	1.88	–1.48	9.6	0.95	185
A9 (2)	×	×	×	25.5	1.74	–1.36	9.9	0.94	207
A11 (1)		×	×	22.7	1.90	–1.11	10.0	0.89	162
A11 (2)	×	×		22.7	1.84	–1.20	10.0	1.12	129
A14 (1)				18.7	1.91	–0.58	10.4	1.37	77
A14 (2)	×	×	×	18.7	1.79	–1.56	10.0	1.03	147
A16 (1)				15.9	1.88	–0.90	9.8	1.08	114
A18 (1)		×		13.5	1.93	–0.81	10.3	1.34	76
A18 (2)	×	×		13.5	2.10	–0.39	10.3	1.48	57
A22 (1)		×		9.5	2.08	–0.65	9.8	1.39	67
A22 (2)	×	×		9.5	1.98	–1.12	10.3	1.31	90
A25 (1)		×		6.7	2.08	–0.44	9.5	1.42	45
A25 (2)	×	×		6.7	1.89	–0.70	10.1	1.31	71
A28 (1)		×		3.5	2.11	–0.38	11.4	1.46	68
A28 (2)	×			3.5	1.86	–1.29	10.5	1.19	126

Note that sample A2 (1) and A2 (2) are from the same specimen, resulting in 25 data points. In terms of the SEM-based optical preservation assessment, six of the 20 brachiopods are considered to be altered.

2). The LO of five of these was used to subdivide the succession into four of the main Upper Cretaceous (UC) biozones applied to the Boreal Province (BP) by Burnett (1998) and to the North Sea by Fritsen (1999) (Figs 3, 6; Table 2). The LO of *Reinhardtites anthophorus*, defining the base of UC16iii of Fritsen (1999), is recorded in the lowermost part of the succession (4.0 m) within the *spinosa-subtilis* zone of Surlyk (1984) (Fig. 3; Table 2). The LO of *Broinsonia parca constricta* (16.0 m), defining the base of UC17, is also encountered within the *spinosa-subtilis* zone. The LO of *Tranolithus orionatus* (24.0 m) lies within the *subtilis-pulchellus* zone and defines the base of UC18. The LOs of *Reinhardtites levis* and *Zeugrhabdotus bicrescenticus* coincide with a minor hardground at 34.0 m (Figs 2, 3) and do not allow differentiation of UC19i and UC19ii, thus representing an unconformity corresponding to the missing UC19i. The LOs of *R. levis* and *Z. bicrescenticus* are thus considered to define the base of UC19ii, which is entirely encompassed by the *pulchellus-pulchellus* zone. In addition, their LOs coincide with the LO of *Prediscosphaera mgayae*. The Hvidskud succession thus encompasses the Boreal nannofossil zones UC16ii – UC19ii (Figs 3, 6).

Bulk rock stable isotope results

A total of 82 bulk rock samples were analysed. The resulting $\delta^{13}C$ curve (Fig. 3) is characterised by an overall positive trend superimposed by several positive and negative fluctuations of higher order between 1.6 and 2.1‰. The lowermost part of the succession exhibits a positive excursion from 1.7 to 2.0‰ which is interrupted by a negative shift down to 1.6‰ at 9.0 m. The overlying interval is characterised by a progressive 0.5‰ increase, interrupted by two short-term negative excursions. The remaining part of the succession is characterised by an overall negative excursion from 2.0 to 1.8‰, interrupted by a significant short positive excursion.

The bulk rock oxygen isotope trend (Fig. 3) is characterised by an overall 0.2‰ decrease, with superimposed higher order positive and negative oscillations between –2.2 to –1.4‰. A five-point moving average was applied to the $\delta^{18}O$ data in order to highlight possible fluctuations and inflection points in the succession (Fig. 3).

A cross-plot of carbon and oxygen isotopes (Fig. 8) allows testing of diagenetic imprints which may result in a positive correlation (Jenkyns *et al.* 1995; Mitchell *et al.* 1997). The absence of a significant correlation in the bulk rock data suggests a relatively low impact of diagenesis.

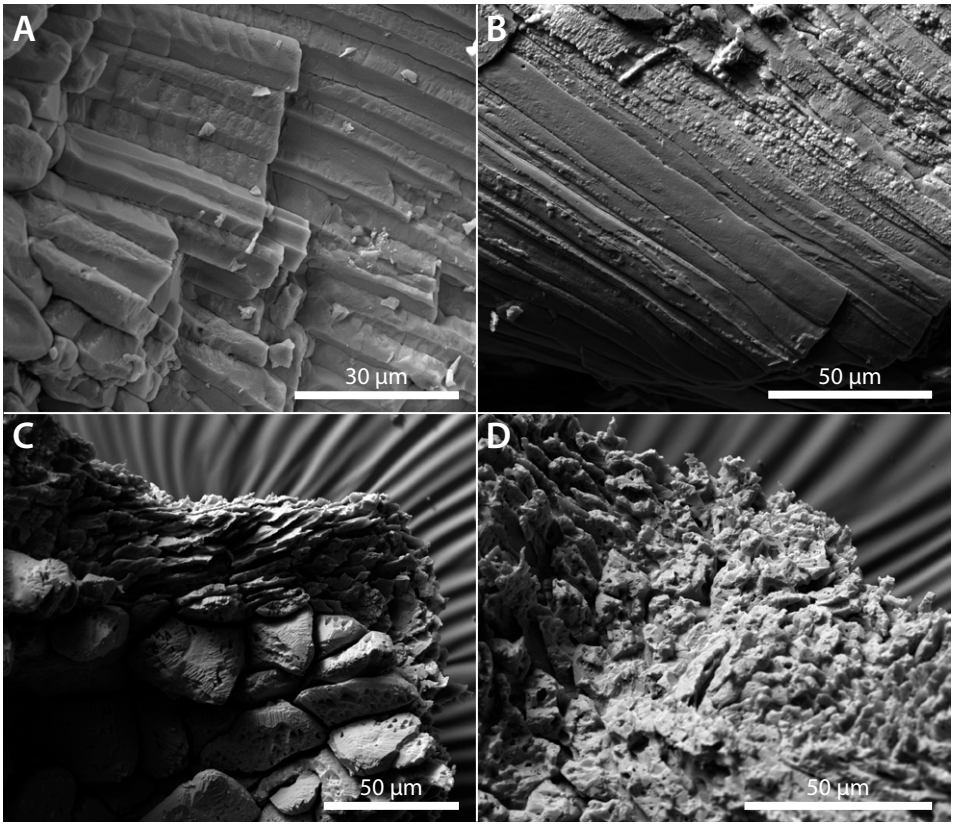

Fig. 7. Representative SEM pictures of four of the 24 leached brachiopod valves, showing (A–B) well-preserved secondary shell layers and (C–D) altered shell material. Regarding the SEM-based preservation assessment only, the shells are generally well-preserved and leaching has successfully removed the main part of the primary layer with only minor exceptions. **A**: A18 (2), 13.5 m. **B**: A25 (1), 6.7 m. **C**: A9 (1), 25.5 m. **D**: A9 (2), 25.5 m.

Screenings, trace element and stable isotope results for brachiopods

Binocular and SEM screenings show that the ultrastructures such as smooth surfaces and anvil-shaped crystals of the fibrous and lamellar structures of the secondary layers of most of the brachiopods are well-preserved (Fig. 7). Features resulting from the leaching process are ignored in this consideration. Six specimens show signs of diagenetic dissolution resulting in irregular surfaces. These specimens are considered to be altered (Fig. 7; Table 4). From the SEM images it can also be concluded that the leaching of the brachiopods has successfully removed the primary shell layers and adhered chalk.

The stable isotope values from the brachiopods are on average heavier than those of the bulk samples (Figs 3, 8). The brachiopod $\delta^{13}C$ trend shows a slight decline of ~0.2‰ (2.0 to 1.8‰) between 3.5 and 18.7 m, and a subsequent ~0.2‰ incline with a short-lived positive excursion (2.1‰) at 31.5 m. The brachiopod $\delta^{18}O$ trend shows a similar trend in the lower and upper part of the succession, and an overall negative excursion between 3.5 and 28.3 m with a change of –1.6‰ and the lightest value down to –2.0‰.

A cross-plot of the carbon and oxygen isotope values reveals a weak positive correlation (Fig. 8), which might indicate diagenetic alteration of the brachiopod shells (cf. Jenkyns *et al.* 1995; Mitchell *et al.* 1997).

Mg/Ca ratios range from 9.3 to 11.4 mmol/mol with an average of 10.1 mmol/mol. Sr/Ca ratios range from 0.89 to 1.48 mmol/mol and are strongly negatively correlated with Mn/Ca ratios that range from 45 to 207 µmol/mol ($r^2 = 0.88$) (Fig. 9). Negative correlations of Mn/Ca with $r^2 > 0.5$ are also observed for $\delta^{13}C$ and $\delta^{18}O$ (Fig. 9).

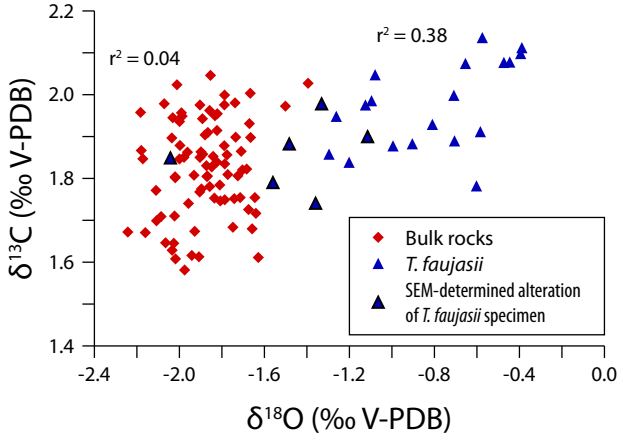

Fig. 8. Cross-plot of carbon and oxygen isotope ratios in bulk samples, showing no significant correlation, and in the micromorphic brachiopod *Terebratulina faujasii*, showing a weak positive correlation. Note the relatively light stable isotope values of the brachiopod specimens considered to be altered from the SEM-based preservation assessment.

Discussion

Diagenetic impact on brachiopod isotopic data

The strong negative correlations of Sr/Ca with Mn/Ca and $\delta^{18}O$ with Mn/Ca point to an important diagenetic imprint on the brachiopods (cf. Brand & Veizer 1981). Significantly, the six specimens that are considered to be altered by means of the SEM-based preservation assessment, are also the specimens with highest Mn/

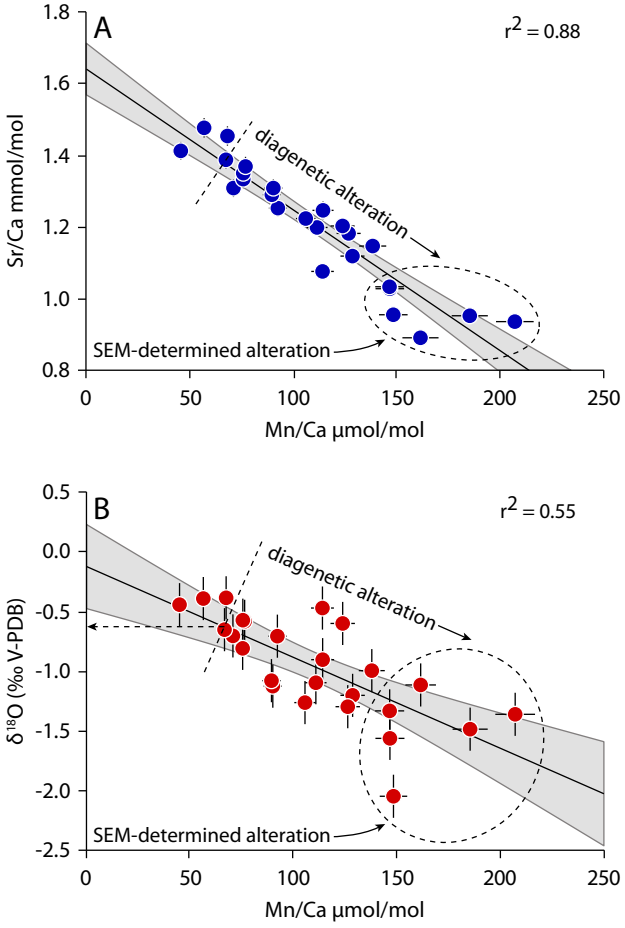

Fig. 9. Cross-plots of geochemical data for the micromorphic brachiopod *Terebratulina faujasii*. **A**: Co-variation of Sr/Ca ratios with Mn/Ca ratios. **B**: Co-variation of $\delta^{18}O$ values with Mn/Ca ratios. Brachiopod values corresponding to the upper-left of the correlation lines indicate the least altered specimens and probably reflect primary bottom water $\delta^{18}O$ values. By discarding the samples that are considered to be altered, it is evident that any $\delta^{18}O$ value lower than –0.6‰ cannot be interpreted with confidence as primary (B). Additionally, in each of the cross-plots, the specimens considered to be altered by means of SEM inspection are more or less clustered in the lower right corner with the highest Mn/Ca ratios (A–B), lowest Sr/Ca ratios (A), and some of the lightest $\delta^{18}O$ values (B), clearly signifying their degree of diagenetic alteration.

Ca ratios, the lowest Sr/Ca ratios (Fig. 9) and some of the lightest stable isotope values (Figs 3, 8; Table 4). Therefore, long-term trends in brachiopod $\delta^{18}O$ cannot be interpreted here. However, it can be inferred that values corresponding to the upper-left of the correlation lines point to the least altered values and probably reflect near to primary bottom water $\delta^{18}O$ values (Fig. 9).

Correlation of brachiopod and nannofossil zonations with carbon isotope stratigraphy

Carbon isotope records have proved to be a powerful tool for stratigraphic correlation (Gale *et al.* 1993; Tsikos *et al.* 2004; Voigt *et al*. 2010, 2012; Batenburg *et al.* 2012; Thibault *et al*. 2012a, b). Calibrating $\delta^{13}C$ curves with detailed biostratigraphic information additionally improves the stratigraphic reliability and helps to correlate biostratigraphic schemes between different palaeobiogeographic realms (Thibault *et al.* 2012a, b). The bulk $\delta^{13}C$ excursions of the Hvidskud succession, together with the nannofossil biostratigraphy, can be used for this purpose. A similar succession of nannofossil bio-events has been found in the upper Campanian – Maastrichtian Stevns-1 core, Stevns Klint, eastern Denmark (Fig. 1), from which a standard $\delta^{13}C$ curve was established for the Boreal Realm (Thibault *et al.* 2012a; Surlyk *et al*. 2013). The Stevns-1 core was drilled only 30 km from Møns Klint and displays an almost identical sequence of nannofossil bio-events from the LO of *R. anthophorus* when compared with Hvidskud (Fig. 10; Thibault *et al*. 2012a). The only exception is that the LO of *Z. bicrescenticus* occurs stratigraphically slightly higher in Stevns-1 than the coincident LOs of *R. levis* and *P. mgayae*. This is in contrast to the Hvidskud succession where the LOs of these three species are coincident (Fig. 10). The three bio-horizons occur at the hardground at 34.0 m, suggesting that the UC19i subzone is missing at Hvidskud (Figs 3, 10).

The $\delta^{13}C$ records of Hvidskud and Stevns-1 are correlated and calibrated by the nannofossil bio-events, allowing the establishment of a precise $\delta^{13}C$ stratigraphy for the Hvidskud succession (Fig. 10). The Stevns-1 core was sampled at a much higher resolution than the Hvidskud succession, and ambiguities in the correlation of the $\delta^{13}C$ profiles may thus exist. However, the correlation is strongly supported by a precise correlation of nannofossil bio-horizons between the two sites. The LO of *R. anthophorus* in both successions allows correlation of the lowermost part of the Hvidskud succession with Stevns-1. The lowermost 0.3‰ increase in the Hvidskud succession corresponds to the short-lived 0.2‰ positive excursion of the M1+ $\delta^{13}C$ event in Stevns-1 (Thibault *et al.* 2012a), and occurs within UC16d^{BP} of Burnett (1998) and the *spinosa-subtilis* zone of Surlyk (1984). The onset of event M1– is marked by an abrupt negative excursion in both successions and the top of this event coincides with the LO of *T. orionatus* (base of UC18). The M1– $\delta^{13}C$ event thus corresponds to the upper part of *spinosa-subtilis* and the lowermost part of *subtilis-pulchellus* brachiopod zones of Surlyk (1984). The LO of *B. parca constricta* is recorded within M1– in both successions (Thibault *et al.* 2012a) (Fig. 10). The overlying part of the Hvidskud succession can only be correlated with confidence on the basis of nannofossil bio-events. The LOs of *P. mgayae*, *R. levis* and *Z. bicrescenticus* appear concomitantly in the level of the hardground-related unconformity and thus confirm omission in this level. Their last occurrences, however, coincide with a significant negative $\delta^{13}C$ excursion in both successions, which can be used as a tie-point to subdivide the M2+ event in the uppermost part of the Hvidskud succession. The M2+ $\delta^{13}C$ event extends from the LO of *T. orionatus* and is comprised by UC18 and UC19 and the *subtilis-pulchellus* and *pulchellus-pulchellus* brachiopod zones (Fig. 10). As in the lowermost part of the succession, the relatively low sampling resolution, compared to that of Stevns-1, prohibits further correlation between the top of the Hvidskud succession and Stevns-1. The Hvidskud succession thus encompasses $\delta^{13}C$ events M1+ to M2+ of Thibault *et al.* (2012a).

The Maastrichtian Stage has recently been astronomically calibrated, and a precise geochronological age model has been proposed (e.g. Husson *et al.* 2011, 2012; Batenburg *et al.* 2012; Thibault *et al.* 2012b). In particular, an integrated framework of magnetostratigraphy, micro- and nannofossil biostratigraphy, cyclostratigraphy and $\delta^{13}C$ stratigraphy was established for the upper Campanian – Maastrichtian succession of Ocean Drilling Program (ODP) Site 762C, Leg 122, drilled in the western part of the central Exmouth Plateau off north-western Australia, eastern Indian Ocean (Galbrun 1992; Husson *et al.* 2011, 2012; Thibault *et al.* 2012b). This site was characterised by nearly continuous pelagic to hemipelagic sedimentation, allowing counting of cycles based on colour changes in the core and thereby the development of a cyclostratigraphic framework. The duration of each magnetochron encountered in the core was inferred from cycle counting, using an age of 66 Ma for the K–Pg boundary (Husson *et al.* 2011, 2012). ODP Site 762C thus constitutes a solid basis for large-scale correlations of the upper Campanian – Maastrichtian interval.

Sedimentation at the Indian Ocean ODP site took place within a mid-latitude, transitional calcareous plankton province of the southern hemisphere. Thibault *et al.* (2012b) noticed that many Maastrich-

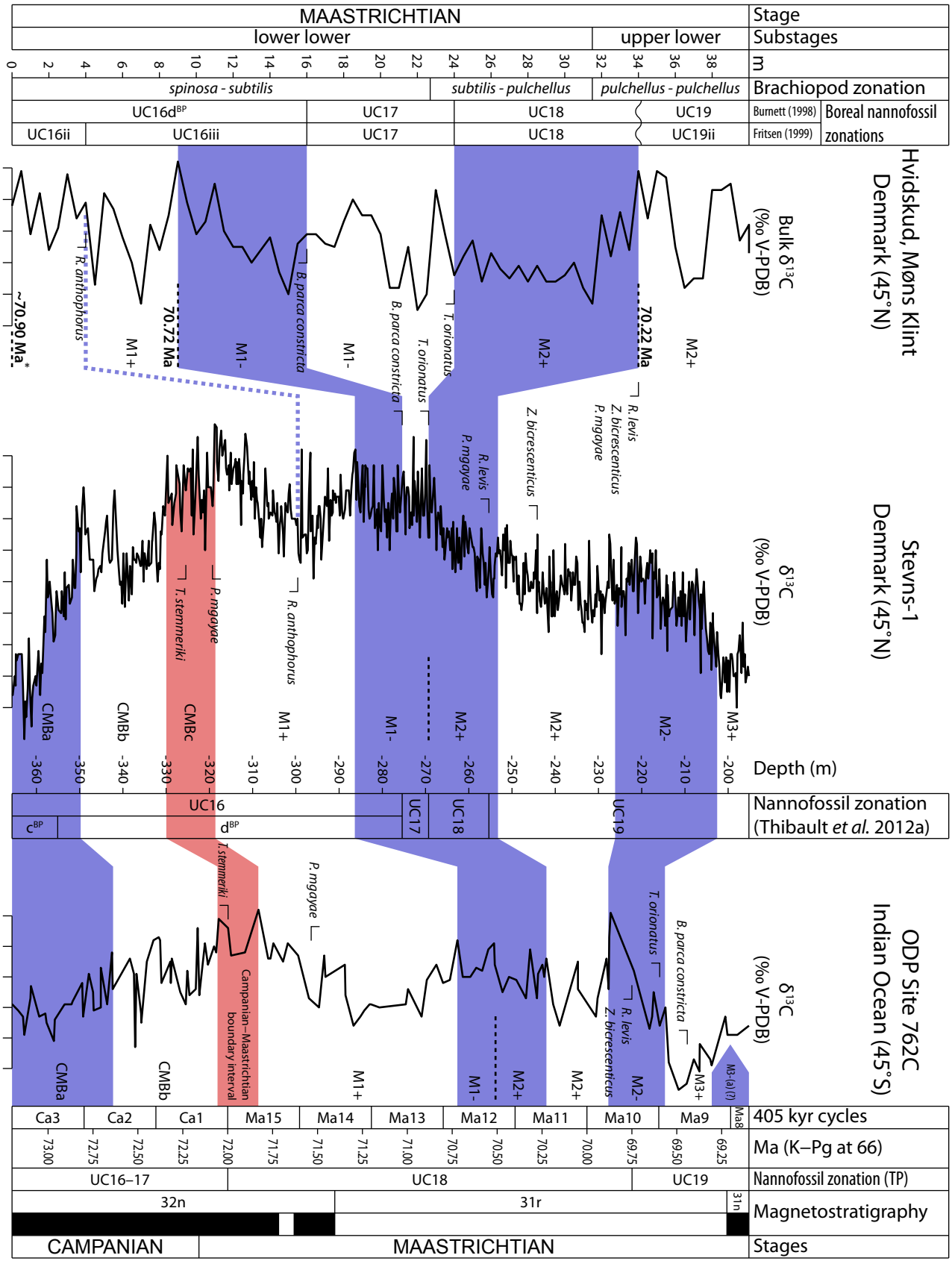
MAASTRICHTIAN
lower lower
upper lower
Stage
Substages
m
Brachiopod zonation
spinosa - subtilis
subtilis - pulchellus
pulchellus - pulchellus
UC16d^BP
UC17
UC18
UC19
Burnett (1998)
Boreal nannofossil zonations
UC16ii
UC16iii
UC17
UC18
UC19ii
Fritsen (1999)
Hvidskud, Møns Klint
Denmark (45°N)
Bulk δ13C (‰ V-PDB)
~70.90 Ma*
70.72 Ma
70.22 Ma
R. anthophorus
B. parca constricta
T. orionatus
R. levis
Z. bicrescenticus
P. mgayae
M1+
M1-
M2+
M2-
Stevns-1
Denmark (45°N)
δ13C (‰ V-PDB)
T. stemmeriki
P. mgayae
R. anthophorus
Z. bicrescenticus
CMBa
CMBb
CMBc
M3+
Depth (m)
Nannofossil zonation (Thibault et al. 2012a)
UC16
UC17
UC18
UC19
c^BP
d^BP
ODP Site 762C
Indian Ocean (45°S)
δ13C (‰ V-PDB)
Campanian–Maastrichtian boundary interval
M3-(a) (?)
Ma8
405 kyr cycles
Ca3
Ca2
Ca1
Ma15
Ma14
Ma13
Ma12
Ma11
Ma10
Ma9
Ma (K–Pg at 66)
Nannofossil zonation (TP)
UC16–17
UC18
UC19
Magnetostratigraphy
32n
31r
31n
CAMPANIAN
MAASTRICHTIAN
Stages

tian calcareous nannofossil bio-events were time-transgressive between this southern province and the Tethyan and Boreal realms. The $\delta^{13}C$ record for ODP 762C is, however, remarkably similar to that of Stevns-1 (Fig. 10; Thibault *et al*. 2012b). Stevns-1 can therefore be used as a reference curve for correlation of the Hvidskud succession with ODP 762C. This allows further chronostratigraphic constraints for the age model of the Hvidskud succession.

A precise correlation of the M1+ $\delta^{13}C$ event between Hvidskud and ODP 762C is not possible, as the correlation between Hvidskud and Stevns-1 in this interval is solely based on the LO of *R. anthophorus* (Fig. 10). The same problem applies in the upper part of the M2+ event above the LOs of *R. levis*, *Z. bicrescenticus* and *P. mgayae*. The M1– and M2+ events up until the LOs of *R. levis*, *Z. bicrescenticus* and *P. mgayae* can, however, be confidently correlated between the successions, allowing construction of an age model for this interval. Calibration to the ODP 762C profile reliably suggests a geochronological duration of this 25 m thick interval of 70.72 Ma – 70.22 Ma, encompassing the 405 kyr eccentricity cycles $Ma_{405}12$ – $Ma_{405}11$ within magnetochron C31r and nannofossil zone UC18 of the Transitional Province (cf. Husson *et al.* 2011; Thibault *et al*. 2012b). This corresponds to an inferred sedimentation rate of 5.0 cm kyr^{-1} (Fig. 10). Assuming that the sedimentation rate was largely uniform throughout, it can be used to calculate an estimated age for the base of the Hvidskud succession on the basis of its thickness. An age for the top of the succession cannot be determined due to the hiatus represented by the hardground unconformity at 34.0 m. The Hvidskud succession extends from ~70.90 Ma to at least 70.22 Ma, thus covering a time interval of at least 680 kyr (Fig. 10).

Climatic implications

The Maastrichtian was characterised by an overall long-term global cooling, superimposed by pronounced climate and temperature fluctuations (Li & Keller 1998a, b, 1999; Barrera & Savin 1999; Thibault & Gardin 2006, 2007). In the early Maastrichtian, the temperature of intermediate water masses decreased globally by 5–6°C, while sea-surface temperatures in mid and high latitudes decreased by 4–5°C. This cooling event was followed by a mid-Maastrichtian warming of 2–3°C in low and mid-latitudes with warmer but fluctuating temperatures continuing from the late part of chron C31r until the base of C30n. The late Maastrichtian was characterised by another global cooling event, followed by the end-Maastrichtian Deccan greenhouse warming (Li & Keller 1998a, 1999; Barrera & Savin 1999; Thibault & Gardin 2006, 2007, 2010).

The age model suggests that the Hvidskud succession correlates with the early Maastrichtian cooling event (cf. Barrera & Savin 1999; Thibault & Gardin 2006). Cool sea-surface temperatures are supported by a relatively common abundance of the calcareous nannofossil cool-water indicators *Ahmuellerella octoradiata* and *Kamptnerius magnificus* throughout the entire Hvidskud succession. This finding was also noted in the calcareous nannofossil assemblage of the Stevns-1 and Skælskør-1 drill cores (eastern Denmark) in the same stratigraphic interval (unpublished data of N. Thibault).

A slight trend towards warmer temperatures in the uppermost part of the succession may be indicated by an overall small decrease in bulk $\delta^{18}O$ values, suggesting that the top of the succession may correspond to the onset of the mid-Maastrichtian warming event. This inference, however, is tentative.

Brachiopods have proved to be a valuable resource in the reconstruction of past seawater temperatures, partly because their low-Mg calcite shells are relatively resistant to diagenetic alteration and because of the possibility of identifying altered samples (e.g. Veizer *et al.* 1999; Korte *et al.* 2005a, b, 2008). In the Hvidskud succession, the strong co-variation of Sr/Ca with Mn/Ca is indicative of a diagenetic trend (Brand & Veizer 1981). It is noticeable that the lightest $\delta^{18}O$ values in brachiopods are close to bulk $\delta^{18}O$ values (Figs 3, 8). Considering that the calcareous nannofossil assemblage points to some degree of diagenesis, as suggested from the microscope-based preservation assessment (Table 2), it is possible that a relatively warm or hyposaline diagenetic fluid impacted both brachiopod and bulk carbonates in the succession. For this reason, it is not reasonable to interpret bulk $\delta^{18}O$ data in further detail.

After discarding brachiopod $\delta^{18}O$ values aligned on

◀ Fig. 10. Correlation of $\delta^{13}C$ profiles between the Hvidskud succession, Stevns-1 drill core and ODP Site 762C, allowing correlation of brachiopod- and nannofossil zonations with $\delta^{13}C$ stratigraphy for Hvidskud. Correlation between Hvidskud and Stevns-1 is almost entirely based on the tie of the nannofossil bio-events due to the geographical proximity of the localities. The Hvidskud succession comprises carbon isotope events M1+ to M2+. Calibration to the ODP 762C $\delta^{13}C$ profile together with an inferred sedimentation rate of 5.0 cm kyr^{-1} suggests a geochronological age for the base of Hvidskud of ~70.9 Ma. It is not possible to calculate an age for the top of the succession. Note the diachronism of calcareous nannofossil bio-horizons and biozones between Hvidskud and Stevns-1 (Boreal Realm) and ODP Site 762C (intermediate latitudes of the southern hemisphere). *The calculation of the age of the base of Hvidskud (~70.9 Ma) is based entirely on the assumption that the inferred sedimentation rate was uniform throughout the lower part of the succession and can thus be used for age estimations.

the diagenetic correlation trend (Fig. 9), it appears that the few heaviest brachiopod values of –0.4 to –0.6‰ would represent the least altered signal for bottom water conditions (Figs 3, 9). A good preservation of the shell material in these specimens is also supported by low Mn/Ca ratios of ~50 μmol/mol and by the SEM screening which reveals that the shells are among the best preserved with well-preserved calcitic layered structures (Fig. 7). This near-pristine range of values (Fig. 3) may thus be used to estimate the minimum palaeotemperature of bottom waters of the Chalk Sea in the Danish Basin. Using the equation of Anderson and Arthur (1983) and a seawater $\delta^{18}O$ of –1‰ for a Late Cretaceous ice-free world, these heaviest brachiopod $\delta^{18}O$ values translate to a range of 13.6 to 14.3°C for bottom waters of the Chalk Sea during the early Maastrichtian cooling, at a palaeolatitude of *c*. 45°N. These palaeotemperature estimates may however be biased by the postulated presence of a small Antarctic ice cap at that time (Barrera & Savin 1999; Gallagher *et al*. 2008; Bowman *et al*. 2013).

Conclusions

A new nannofossil and $\delta^{13}C$ stratigraphy is established for the Hvidskud succession and correlated with the brachiopod zonation of Surlyk (1984). A chronostratigraphic and geochronological age model is proposed for the succession on the basis of correlation with the cored boreholes Stevns-1 and ODP Site 762C. Seawater temperatures are additionally inferred from combined bulk rock and brachiopod stable isotope data together with the distribution of calcareous nannofossils, brachiopod trace elements and SEM data.

The Hvidskud succession encompasses the Boreal nannofossil zones UC16ii to UC19ii within the lower Maastrichtian. These nannofossil zones are now tied to the brachiopod zonation.

Carbon isotope stratigraphy of the Hvidskud succession and correlation with the Stevns-1 core allow recognition of $\delta^{13}C$ events M1+ to M2+. The correlation of Hvidskud with Stevns-1 and the tie of this interval to the astronomically calibrated ODP Site 762C constrains an age of ~70.9 Ma for the base of the succession. The succession extends across the 405 kyr eccentricity cycles $Ma_{405}13$ – $Ma_{405}11$ in magnetochron C31r and across the Boreal lower lower and upper lower Maastrichtian boundary. The entire succession covers a time interval of at least 680 kyr, with an average sedimentation rate of 5.0 cm kyr^{-1}.

The chalk of Hvidskud was deposited during the early Maastrichtian cooling period and bulk oxygen isotope values remain relatively stable in the studied interval. A slight trend towards lighter values towards the top of the succession may represent the onset of the mid-Maastrichtian warming. Most brachiopod $\delta^{18}O$ values point to an impact of diagenesis. Near-pristine shell values can be narrowed to a range of –0.4 to –0.6‰. Considering a Late Cretaceous ice-free world, these values translate into a range of temperatures of 13.6 to 14.3°C for bottom waters of the Danish Chalk Sea (45°N) during the early Maastrichtian cooling episode. These estimates may however require correction if the presence of continental ice in Antarctica during the Maastrichtian is confirmed in the future.

Acknowledgements

The study was funded by the Carlsberg Foundation. Bo Petersen kindly provided technical support. We thank journal reviewers Emma Sheldon and Erik Thomsen as well as editor Jan Audun Rasmussen for constructive comments and corrections.

References

Anderskouv, K. & Surlyk, F. 2011: Upper Cretaceous chalk facies and depositional history recorded in the Mona-1 core, Mona Ridge, Danish North Sea. Geological Survey of Denmark and Greenland Bulletin 25, 60 pp.

Anderson, T.F. & Arthur, M.A. 1983: Stable isotopes of oxygen and carbon and their application to sedimentological and palaeoenvironmental problems. In: Arthur, M.A. *et al*. (eds): Stable Isotopes in Sedimentary Geochemistry. Society of Economic Palaeontologists and Mineralogists Short Course 10, 111–151.

Barrera, E. & Savin, S.M. 1999: Evolution of late Campanian–Maastrichtian marine climates and oceans. Geological Society of America Special Papers 332, 245–282.

Batenburg, S.J. *et al*. 2012: Cyclostratigraphy and astronomical tuning of the Late Maastrichtian at Zumaia (Basque country, Northern Spain). Earth and Planetary Science Letters 359–360, 264–278.

Birkelund, T. 1957: Upper Cretaceous Belemnites from Denmark. Det Kongelige Danske Videnskabernes Selskab, Biologiske Skrifter 9, 69 pp.

Bowman, V.C., Francis, J.E. & Riding, J.B. 2013: Late Cretaceous winter sea ice in Antarctica? Geology 41, 1227–1230.

Brand, U. & Veizer, J. 1981: Chemical diagenesis of a multicomponent carbonate system; 2, Stable isotopes. Journal of Sedimentary Research 51, 987–997.

Burnett, J. 1998: Upper Cretaceous. In: Bown, P.R. (ed.): Calcareous Nannofossil Biostratigraphy. Chapman and Hall/Kluwer Academic Publishers, London, 132–199.

Carpenter, S.J. & Lohmann, K.C. 1995: $\delta^{18}O$ and $\delta^{13}C$ values of modern brachiopod shells. Geochimica et Cosmochimica Acta 59, 3749–3764.

Esmerode, E.V., Lykke-Andersen, H. & Surlyk, F. 2008: Interaction between bottom currents and slope failure in the Late Cretaceous of the southern Danish Central Graben, North Sea. Journal of the Geological Society, London 165, 55–72.

Fritsen, A. 1999: A Joint Chalk Stratigraphic Framework. In: Joint Chalk Research Program Topic V. Volume 1. Norwegian Petroleum Directorate, 206 pp.

Galbrun, B. 1992: Magnetostratigraphy of Upper Cretaceous and lower Tertiary sediments, Sites 761 and 762, Exmouth Plateau, northwest Australia. Proceedings of the Ocean Drilling Program, Scientific Results 122, 699–716.

Gale, A.S., Jenkyns, H.C., Kennedy, W.J. & Corfield, R.M. 1993: Chemostratigraphy versus biostratigraphy: data from around the Cenomanian–Turonian boundary. Journal of the Geological Society, London 150, 29–32.

Gallagher, S.J., Wagstaff, B.E., Baird, J.G., Wallace, M.W. & Li, C.L. 2008: Southern high latitude climate variability in the Late Cretaceous greenhouse world. Global and Planetary Change 60, 351–364.

Griesshaber, E., Schmahl, W.W., Neuser, R., Pettke, T., Blüm, M., Mutterlose, J. & Brand, U. 2007: Crystallographic texture and microstructure of terebratulide brachiopod shell calcite: an optimized materials design with hierarchical architecture. American Mineralogist 92, 722–734.

Haq, B.V., Hardenbol, J. & Vail, P.R. 1988: Mesozoic and Cenozoic chronostratigraphy and cycles of sea-level change. In: Wilgus, C.K. *et al.* (eds): Sea-level Changes; an Integrated Approach. Society of Economic Paleontologists and Mineralogists (SEPM) Special Publication 42, 71–108.

Husson, D., Galbrun, B., Laskar, J., Hinnov, L., Thibault, N., Gardin, S. & Locklair, R.E. 2011: Astronomical calibration of the Maastrichtian (late Cretaceous). Earth and Planetary Science Letters 305, 328–340.

Husson, D., Galbrun, B., Thibault, N., Gardin, S., Huret, E. & Coccioni, R. 2012: Astronomical duration of polarity Chron C31r (Lower Maastrichtian): cyclostratigraphy of ODP Site 762 (Indian Ocean) and the Contessa Highway section (Gubbio, Italy). Geological Magazine 149, 345–351.

Håkansson, E. & Surlyk, F. 1997: Denmark. In: Moores, E.M. & Fairbridge, R.W. (eds): Encyclopedia of European and Asian Regional Geology. Chapman & Hall, 183–192.

Imai, N., Terashima, S., Itoh, S. & Ando, A. 1996: 1996 compilation of analytical data on nine GSJ geochemical reference samples, "Sedimentary rock series". Geostandards Newsletter 20, 165–216.

Jenkyns, H.C., Mutterlose, J. & Sliter, W.V. 1995: Upper Cretaceous carbon- and oxygen-isotope stratigraphy of deep-water sediments from the North-Central Pacific (Site 869, Flank of Pikinni-Wodejebato, Marshall Islands). Proceedings of the Ocean Drilling Program, Scientific Results 143, 105–108.

Johansen, M.B. & Surlyk, F. 1990: Brachiopods and the stratigraphy of the Upper Campanian and Lower Maastrichtian chalk of Norfolk, England. Palaeontology 33, 823–873.

Koch, C. & Young, J.R. 2007: A simple weighing and dilution technique for determining absolute abundances of coccoliths from sediment samples. Journal of Nannoplankton Research 29, 67–69.

Kominz, M.A., Browning, J.V., Miller, K.G., Sugarman, P.J., Mizintsevat, S. & Scotese, C.R. 2008: Late Cretaceous to Miocene sea-level estimates from the New Jersey and Delaware coastal plain coreholes: an error analysis. Basin Research 20, 211–226.

Korte, C., Jasper, T., Kozur, H.W. & Veizer, J. 2005a: $\delta^{18}O$ and $\delta^{13}C$ of Permian brachiopods: a record of seawater evolution and continental glaciations. Palaeogeography, Palaeoclimatology, Palaeoecology 224, 333–351.

Korte, C., Kozur, H.W. & Veizer, J. 2005b: $\delta^{13}C$ and $\delta^{18}O$ values of Triassic brachiopods and carbonate rocks as proxies for coeval seawater and palaeotemperature. Palaeogeography, Palaeoclimatology, Palaeoecology 226, 287–306.

Korte, C., Jones, P.J., Brand, U., Mertmann, D. & Veizer, J. 2008: Oxygen isotope values from high-latitudes: Clues for Permian sea-surface temperature gradients and Late Palaeozoic deglaciation. Palaeogeography, Palaeoclimatology, Palaeoecology 269, 1–16.

Li, L. & Keller, G. 1998a: Maastrichtian climate, productivity and faunal turnovers in planktic foraminifera in South Atlantic DSDP sites 525A and 21. Marine Micropaleontology 33, 55–86.

Li, L. & Keller, G. 1998b: Abrupt deep-sea warming at the end of the Cretaceous. Geology 26, 995–998.

Li, L. & Keller, G. 1999: Variability in Late Cretaceous climate and deep waters: evidence from stable isotopes. Marine Geology 161, 171–190.

Liboriussen, J., Ashton, P. & Tygesen, T. 1987: The tectonic evolution of the Fennoscandian Border Zone. Tectonophysics 137, 21–29.

Mitchell, S.F., Ball, J.D., Crowley, S.F., Marshall, J.D., Paul, C.R.C., Veltkamp, C.J. & Samir, A. 1997: Isotope data from Cretaceous chalks and foraminifera: environmental or diagenetic signals? Geology 25, 691–694.

Mogensen, T.E. & Korstgård, J.A. 2003: Triassic and Jurassic transtension along part of the Sorgenfrei–Tornquist Zone in the Danish Kattegat. In: Ineson, J.R. & Surlyk, F. (eds): The Jurassic of Denmark and Greenland. Geological Survey of Denmark and Greenland Bulletin 1, 439–458.

Parkinson, D., Curry, G.B., Cusack, M. & Fallick, A. 2005: Shell structure, patterns and trends of oxygen and carbon stable isotopes in modern brachiopod shells. Chemical Geology 219, 193–235.

Rasmussen, S.L. & Surlyk, F. 2012: Facies and ichnology of an Upper Cretaceous chalk contourite drift complex, eastern Denmark, and the validity of contourite facies models. Journal of the Geological Society, London 169, 435–447.

Roth, P.H. 1983: Jurassic and Lower Cretaceous calcareous nannofossils in the western North Atlantic (Site 543): biostratigraphy, preservation and some observation on

biogeography and paleoceanography. Initial Reports of the Deep Sea Drilling Project 76, 587–621.

Schulz, M.-G. 1979: Morphometrisch-variationsstatistische Untersuchungen zur Phylogenie der Belemniten-Gattung *Belemnella* im Untermaastricht NW-Europas. Geologisches Jahrbuch A 47, 3–157.

Steinich, G. 1965: Die artikulaten Brachiopoden der Rügener Schreibkreide (Unter-Maastricht). Paläontologische Abhandlungen A 2, 1–220.

Stemmerik, L., Surlyk, F., Klitten, K., Rasmussen, S.L. & Schovsbo, N. 2006: Shallow core drilling of the Upper Cretaceous Chalk at Stevns Klint, Denmark. Geological Survey of Denmark and Greenland Bulletin 10, 13–16.

Stenestad, E. 1972: Træk af det danske bassins udvikling i Øvre Kridt. Dansk Geologisk Forenings Årsskrift for 1971, 63–69.

Surlyk, F. 1969: En undersøgelse over de articulate brachiopoder i det danske skrivekridt (ø. campanien og maastrichtien) med en oversigt over skrivekridtets sedimentologi og skrivekridthavets flora og fauna. Unpublished prize dissertation. University of Copenhagen, 319 pp.

Surlyk, F. 1970: Die Stratigraphie des Maastricht von Dänemark und Norddeutschland aufgrund von Brachiopoden. Newsletters on Stratigraphy 1, 7–16.

Surlyk, F. 1979: Maastrichtian brachiopods from Denmark. In: Birkelund, T. & Bromley, R.G. (eds): Cretaceous – Tertiary Boundary Events, Symposium. The Maastrichtian and Danian of Denmark, University of Copenhagen, 45–50.

Surlyk, F. 1982: Brachiopods from the Campanian–Maastrichtian boundary sequence, Kronsmoor (NW Germany). Geologisches Jahrbuch A 61, 259–277.

Surlyk, F. 1984: The Maastrichtian Stage in NW Europe, and its brachiopod zonation. Bulletin of the Geological Society of Denmark 33, 217–223.

Surlyk, F. & Birkelund, T. 1977: An integrated stratigraphical study of fossil assemblages from the Maastrichtian White Chalk of northwestern Europe. In: Kauffman, E.G. & Hazel, J.E. (eds): Concepts and Methods of Biostratigraphy. Dowden, Hutchinson & Ross, Stroudsburg, 257–281.

Surlyk, F. & Lykke-Andersen, H. 2007: Contourite drifts, moats and channels in the Upper Cretaceous chalk of the Danish Basin. Sedimentology 54, 405–422.

Surlyk, F., Rasmussen, S.L., Boussaha, M., Schiøler, P., Schovsbo, N.H., Sheldon, E., Stemmerik, L. & Thibault, N. 2013: Upper Campanian–Maastrichtian holostratigraphy of the eastern Danish Basin. Cretaceous Research 46, 232–256.

Thibault, N. & Gardin, S. 2006: Maastrichtian calcareous nannofossil biostratigraphy and paleoecology in the Equatorial Atlantic (Demerara Rise, ODP Leg 207 Hole 1258A). Revue de micropaléontologie 49, 199–214.

Thibault, N. & Gardin, S. 2007: The late Maastrichtian nannofossil record of climate change in the South Atlantic DSDP Hole 525A. Marine Micropaleontology 65, 163–184.

Thibault, N. & Gardin, S. 2010: The calcareous nannofossil response to the end-Cretaceous warm event in the Tropical Pacific. Palaeogeography, Palaeoclimatology, Palaeoecology 291, 239–252.

Thibault, N., Harlou, R., Schovsbo, N., Schiøler, P., Minoletti, F., Galbrun, B., Lauridsen, B.W., Sheldon, E., Stemmerik, L. & Surlyk, F. 2012a: Upper Campanian–Maastrichtian nannofossil biostratigraphy and high-resolution carbon-isotope stratigraphy of the Danish Basin: Towards a standard $\delta^{13}C$ curve for the Boreal Realm. Cretaceous Research 33, 72–90.

Thibault, N., Husson, D., Harlou, R., Gardin, S., Galbrun, B., Huret, E. & Minoletti, F. 2012b: Astronomical calibration of upper Campanian–Maastrichtian carbon isotope events and calcareous plankton biostratigraphy in the Indian Ocean (ODP Hole 762C): Implication for the age of the Campanian–Maastrichtian boundary. Palaeogeography, Palaeoclimatology, Palaeoecology 337–338, 52–71.

Tsikos, H. *et al*. 2004: Carbon-isotope stratigraphy recorded by the Cenomanian–Turonian Oceanic Anoxic Event: correlation and implications based on three key localities. Journal of the Geological Society, London 161, 711–719.

Ullmann, C.V., Campell, H.J., Frei, R., Hesselbo, S.P., Pogge von Strandmann, P.A.E. & Korte, C. 2013: Partial diagenetic overprint of Late Jurassic belemnites from New Zealand: Implications for the preservation potential of $\delta^{7}Li$ values in calcite fossils. Geochimica et Cosmochimica Acta 120, 80–96.

Veizer, J. *et al*. 1999: $^{87}Sr/^{86}Sr$, $\delta^{13}C$ and $\delta^{18}O$ evolution of Phanerozoic seawater. Chemical Geology 161, 59–88.

Vejbæk, O.V. & Andersen, C. 2002: Post mid-Cretaceous inversion tectonics in the Danish Central Graben – regionally synchronous tectonic events? Bulletin of the Geological Society of Denmark 47, 139–144.

Voigt, S., Friedrich, O., Norris, R.D. & Schönfeld, J. 2010: Campanian – Maastrichtian carbon isotope stratigraphy: shelf – ocean correlation between the European shelf sea and the tropical Pacific Ocean. Newsletters on Stratigraphy 44, 57–72.

Voigt, S., Gale, A., Jung, C. & Jenkyns, H. 2012: Global correlation of Upper Campanian – Maastrichtian successions using carbon isotope stratigraphy: development of a new Maastrichtian timescale. Newsletters on Stratigraphy 45, 25–53.